Revision 1

The enigma of labradorite feldspar with incommensurately modulated structure, solved

Shiyun Jin and Huifang Xu

NASA Astrobiology Institute, Department of Geoscience, University of Wisconsin–Madison, Madison, Wisconsin 53706

* Corresponding author:
Dr. Huifang Xu, Professor
Department of Geoscience,
University of Wisconsin-Madison
608-265-5887 (O)
hfxu@geology.wisc.edu

Abstract

Intermediate plagioclase feldspars are the most abundant minerals in the earth's crust. Their incommensurately modulated structure has puzzled geologists and crystallographers for decades since the phenomenon in a labradorite was reported in 1940. Solving the structure is a necessary step toward mapping the complex subsolidus phase relations of plagioclase solid solution. The structure of a homogeneous labradorite (An51) single crystal from a metamorphic rock is solved and refined from single crystal X-ray diffraction. The result structure can be simplified as alternating $I1$ lamellae domains related by inversion twin. The inversion boundary shows an anorthite-like structure with $I\bar{1}$ symmetry, and is richer in Ca than the neighboring domains with opposite polarity. No albite-like subunits appear in the *e*-plagioclase structure. The incommensurately modulated structure displays a unique Al-Si ordering pattern. A density modulation with an amplitude of 17 mole% in composition is also observed, and can be properly described only by applying also second order harmonic waves for the atomic modulation functions. The modulated structure reveals details which can't be observed from refinement with only main reflections, and may be use to assess the ordering state and cooling rate of its host rock. The homogeneity of the crystal indicates the closure of the solvus for Bøggild intergrowth at low temperature. The highly ordered modulation supports the thermodynamic stability of *e*-plagioclase. Both Al-Si ordering and Ca-Na ordering are the driving force for formation of the incommensurately modulated structure.

Keywords: Intermediate plagioclase, incommensurate, modulated structure, density modulation, single crystal XRD, *e*-plagioclase, labradorite, aperiodic crystal

Introduction

Plagioclase feldspars, which form a coupled solid solution between albite (Ab: $NaAlSi_3O_8$) and anorthite (An: $CaAl_2Si_2O_8$), are the most abundant group of minerals in the earth's crust, and can be found in most igneous and metamorphic rocks. However, the complicated crystal structure and subsolidus phase relation has been puzzling mineralogists for decades. The most enigmatic feature of plagioclase is the incommensurately modulated or aperiodic structure (*e*-plagioclase) that appears in low plagioclase with composition between ~An25 and ~An75 (Bown and Gay 1959; Ribbe and Hofmeister 1983; Smith and Brown 1988). The crystal structure of *e*-plagioclase has been an enigma since its first discovery in 1940 (Chao and Taylor 1940). Several different models for *e*-plagioclase have been raised over the decades, yet none of them solved the structure satisfactorily. All previous models are based on alternating anorthite domains with antiphase relation to one another, while some display density modulation by inserting albite-like *C* domains in between *I* domains (Cinnamon and Bailey 1971; Grove 1977; Horst et al. 1981; Kumao et al. 1981; McConnell and Fleet 1963; Megaw 1960a, b, c; Nakajima et al. 1977; Smith and Ribbe 1969; Steurer and Jagodzinski 1988; Toman and Frueh 1976a, 1976b; Wenk and Nakajima 1980) (Fig. *1*).

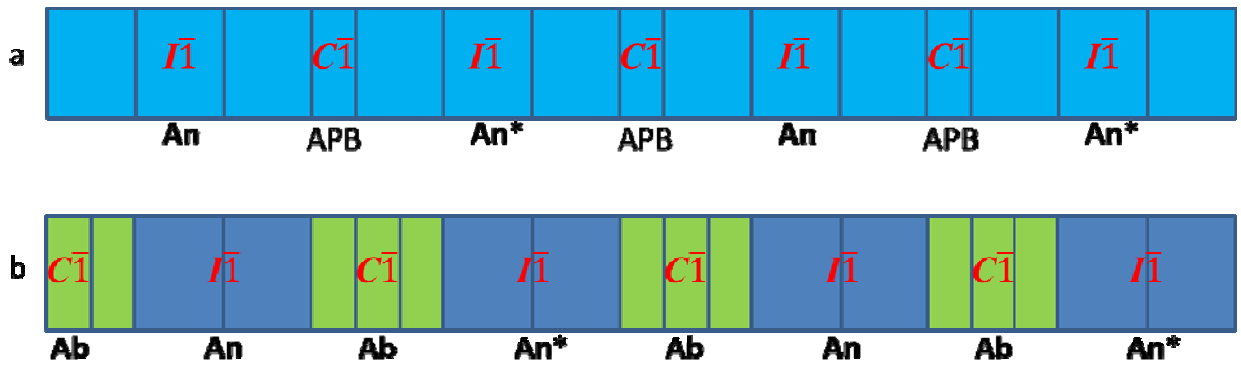

Fig. 1 Previously proposed models for *e*-plagioclase. ***a***. *I* domains separated by antiphase boundaries; ***b***. *I* domains with antiphase relation separated by albite-like *C* domains, the different colors indicate compositional variation.

Most single crystal X-ray analyses of *e*-plagioclase have been done on labradorite (Boysen and Kek 2015; Horst et al. 1981; Toman and Frueh 1976a, 1976b; Yamamoto et al. 1984), with An composition about 50, which is about the middle of entire compositional range of *e*-plagioclase. As the An composition increases, so do the intensities of satellite reflections and the modulation period(Smith and Brown 1988). Labradorite is an ideal specimen as the satellites are separate enough to be easily discerned and strong enough for quality refinement. However, igneous plagioclase of this composition often exhibit iridescent color from the Bøggild intergrowth. All the labradorite samples studied previously actually consist of two phases with different compositions and modulation periods (Boysen and Kek 2015; Horst et al. 1981; Yamamoto et al. 1984), which was considered a serious problem (Ribbe and Hofmeister 1983), because the reflections from the two components overlap and therefore a structure refined to such a diffraction pattern is obviously a composite of two structures of different compositions and can have no real physical meaning. Two totally different structure models for the labradorite were proposed with R values of ~ 10% for *e*-reflections based on the exact same set of diffraction data (Horst et al. 1981; Yamamoto et al. 1984). Boysen and Kek (2015) attempted to solve the problem by introducing another set of satellites from exsolution lamellae, yet they still could not discern the detailed differences between two phases. Their structural refinement was not complete and contained unrealistic occupancies. It is obvious that both good crystal samples (single crystal without exsolution lamellae) and data quality are prerequisites for obtaining an unambiguous structure model with much lower R values for the satellite reflections. A comparison of previous structure refinements and this work is summarized in *Table 1*.

Table 1 Comparison of Structure refinement results

Composition	Publication	Number of reflections	R	parameters
An73	Kitamura and Morimoto 1975, 1977	1072(210*a*+432*e*+430*f*)[a]	0.24	132
An55	Toman and Frueh 1976a, 1976b	1530(720*a*+492*e*+318*f*)	(0.071/0.215/0.27)[b]	307
An52	Horst et al. 1981	4910(1640*a*+3270*e*)	0.08(0.066/0.182)	255
An52	Yamamoto et al. 1984	4910(1640*a*+3270*e*)	0.08(0.066/0.105)	429
An38[c]	Steurer and Jagodzinski 1988	3519(1176*a*+2343*e*)	0.106(0.044/0.33)	216
An52	Boysen and Kek 2015	13518(4354*a*+4535*e*+3069*f*)[d]	0.031(0.023/0.037/0.13)	578
An51	this work	5124(1842*a*+2616*e*+666*f*)	0.024(0.021/0.025/0.06)	642

[a] Letter *a*, *e*, and *f* refer to main reflections, first order satellites, and second order satellites respectively

[b] Values in parentheses refer to R for *a*, *e*, and *f* reflections respectively

[c] The composition was previously reported An63 (Wenk et al. 1980) and corrected to An38 (Smith and Wenk 1983)

[d] There are also 1560 third order satellite observed, with a R of 0.29

All the labradorite samples used for X-ray studies display iridescent color, and are of igneous origin. Grove et al (1983) observed homogenous *e*-labradorite in a metamorphic rock. The composition lies in the compositional range of the Bøggild immiscible gap, and was interpreted by Grove et al (1983) as metastable. However, both early transmission electron microscopy (TEM) observations and our own TEM results do not show any evidence of exsolution in this crystal (*Fig. 2*). With no two phase intergrowth, a low potassium content, and a lack of defects introduced by cooling phase transformations, metamorphic plagioclase is an ideal sample for single crystal X-ray analysis of the modulated structure. Therefore, the data collected on a metamorphic labradorite without exsolution lamellae should provide reliable data towards solving the mysterious structure of the intermediate plagioclase with incommensurately modulated structure, or *e*-plagioclase.

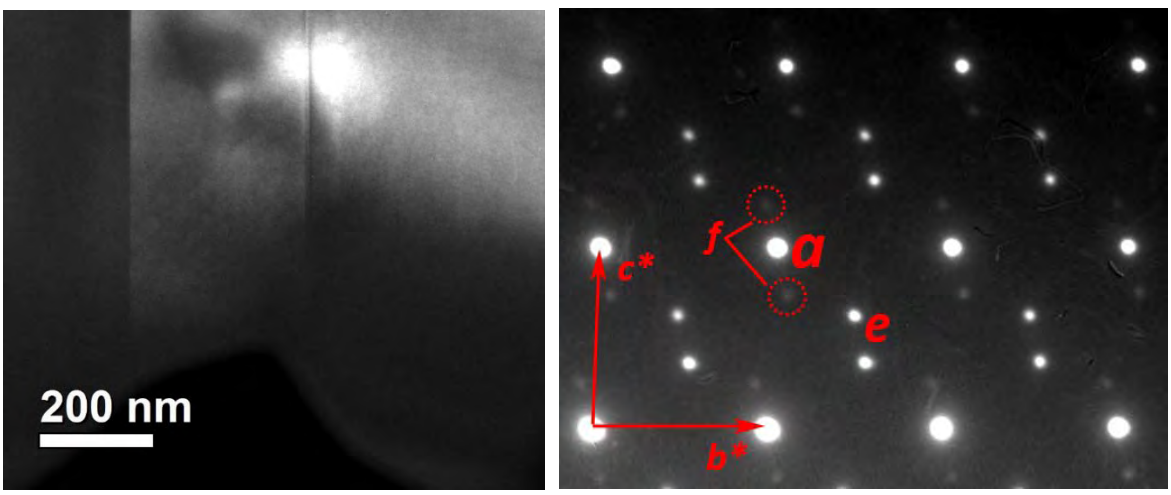

Fig. 2 Dark-field TEM image along ***a***-axis showing albite twin boundary (left); An selected-area electron diffraction pattern showing main *a*-reflections and satellite reflections (*e*- and *f*-reflections). No exsolution lamellae were observed in this crystal.

Sample and Experimental Methods

The sample analyzed in this paper is a labradorite from 987-L (An49-An51) mentioned by Grove et al. (1983). The host rock is a metamorphosed carbonate rock near Augusta, Maine (Ferry 1980). Crystals are smaller than 0.5mm in size and contain both albite twins and pericline twins. The temperature and pressure of metamorphism was calculated as ~530℃ and ~3.6Kbars (Ferry

1980), respectively. The crystal is slightly Ca-rich (An50-An52) with trace amount of K, which is hardly detectable by energy-dispersive spectroscopy (EDS).

Ion milled samples were used in TEM study. A 3mm copper ring was mounted onto a 30μm-thick optical thin section by epoxy, with the area of interest in the center, and then cut off from the thin section and soaked in acetone to eliminate the crystalbond on the sample. The sample was ion milled with a Fischione 1050 at 5.2kV for about 8 hours at 10° angle, and then milled at 1.3kv for another half hour to get rid of the amorphous matter on the sample. The sample was coated with a thin layer of carbon before examined with TEM. TEM images and selected area electron diffraction pattern (SAED) were taken on a Philips CM200UT. Composition of the plagioclase was examined by attached X-ray energy-dispersive spectroscopy (EDS). The EDS result is calibrated using mineral standards of anorthite, labradorite, and orthoclase, composition of which were analyzed by electron microprobe.

The crystal for X-ray diffraction was picked from the thin section and mounted on a glass fiber with epoxy glue. The X-ray diffraction data was collected on a Bruker Quazar APEXII single crystal diffractometer with Mo Kα IμS source at room temperature. 4 ω runs and 1 φ run were programmed with a scan width of 0.5° and a 60 second exposure time. The instrument was running at power of 50kV and 0.6mA. The detector was at a distance of 5cm from the crystal. Unit cell parameter was calculated and refined by APEXII software, as well as peak integration. Absorption correction was done analytically with JANA2006 software (Petříček et al. 2014). The structure was solved with charge flipping algorithm (Oszlanyi and Suto 2004, 2005) using SUPERFLIP (Palatinus and Chapuis 2007). The refinement of the average structure and modulated structure was done with JANA2006 (Petříček et al. 2014) as well. The 3-D crystal structure was visualized by VESTA (Momma and Izumi 2011).

Structure Description

Average Structure

The average structure refined from only main *a* reflections is provided in *Supplementary data*. The average structure is not different from any plagioclase structure with $C\bar{1}$ symmetry, except the T1o site is more concentrated in Al than crystals in volcanic rock (Fitz Gerald et al. 1986).

The refined composition is An52 which matches the EDS results. M2 site is more concentrated in Ca, and M1 more Na. The <T-O> bond distances are 1.6907Å, 1.6508Å, 1.6474Å, 1.6562Å for T1o, T1m, T2o, and T2m respectively. The Al occupancies are estimated by the <T-O> bond distances.

Modulated Structure

Incommensurately modulated structures are quite common in nature, and have been an important subject of crystallography for a long time. Crystallographers observed anomalies in the crystal morphology of modulated structures (Dam et al. 1985; Donnay 1935) even before non-indexable satellite reflections were discovered in X-ray diffraction work (Janner and Janssen 2015). Since the satellite reflections from incommensurate modulated structures cannot be indexed with integers in the traditional way, an extra base has to be introduced for the satellites. As periodicity is lost in real space, the modulation is independent from the subcell edges. Characterization of incommensurately modulated structure in (3+1)D space is a fully developed theory (van Smaalen 2007; Wagner and Schoenleber 2009), and powerful and user- friendly software is available (Petříček et al. 2014). In a (3+1)D structure, each atom isn't simply described by a set of fractional coordination (x, y, z) and a constant occupancy, but a set of periodic modulation functions instead. Actually, each parameter in 3D structure corresponds to a one-dimensional function, the atomic modulation function (AMF), in (3+1)D structure. In this paper, every modulation function is described as a sum of simple harmonic functions of first and second order, with period of unity and half of the modulation period respectively.

The modulated structure was refined in the conventional c=14Å unit cell, since *b* reflections (i.e., $h+k+l=2n$ in the plagioclase) are replaced by satellite *e*-reflections, a special centering condition is applied, namely (½ ½ ½ 0), (0 0 ½ ½), (½ ½ 0 ½). The notation for the (3+1)D space group is $X\bar{1}(\alpha\beta\gamma)0$, corresponding to 2.1.1.1 in the tabulated superspace groups by Stokes et al. (2011). X indicates the unconventional centering condition (C_c' in *Table 3.9* of van Smaalen (2007)) mentioned above and $\bar{1}$ is simply the triclinic point group extended to the (3+1)D hyperspace. (αβγ) means the ***q***-vector has component (i.e., δh, δk, δl in

Table 2) along all three axes in reciprocal space, since there's no symmetrical constraint in a triclinic structure. More basic information about the structure refinement can be found in

Table *2*. Atomic occupancies and positions are listed in *Table 3*. Complete crystallographic information file (cif file) of the refinement can be found in *Supplementary Data*. A movie (*Supplementary Movie 1*) is also provided illustrating how the structure is modulated as function of phase parameter t (the movie displays the stationary modulation wave running through the crystal structure). Though lower case "*t*" is conventionally used for Al contents of T sites in feldspars, in this paper it would only mean the phase parameter of the modulation.

Table 2 Crystallographic information of the labradorite (An51) sample.

Refined composition:	
$Ca_{0.518}Na_{0.482}Si_{2.482}Al_{1.518}O_8$	θ_{min} = 1.94
$X\bar{1}(\alpha\beta\gamma)0$[a]	θ_{max} = 30.54
a = 8.1668(1) Å	θ_{full} = 30.54
b = 12.8509(1) Å	F(000) = 1073
c = 14.2086(2) Å	total reflections: 10168
α = 93.5802(6) °	observed reflections: 5124
β = 116.2300(9) °	main reflections (*a*): 1842
γ = 89.8396(13) °	first order satellite (*e*): 2616
δ*h* = 0.06707(9)	second order satellite (*f*): 666
δ*k* = 0.05463(9)	Refined on F^2
δ*l* = -0.23038(8)	R(obs) [I>3σ(I)] = 0.0235 (2.10%/2.50%/6.14%)[b]
Modulation period: 30.15Å	wR(obs) [I>3σ(I)] = 0.0696 (7.50%/5.23%/12.46%)[b]
Cell Volume: 1334.53(3) $Å^3$	R(all) = 0.0478 (2.29%/4.48%/23.12%)[b]
Z = 8	wR(all) = 0.0718 (7.52%/5.48%/17.54%) [b]
T = 293K	goodness of fit(all) = 1.28
0.058×0.059×0.153mm	goodness of fit(obs) = 1.8
colorless	642 parameters refined

[a] Centering condition X: (½,½,½,0),(½,½,0,½),(0,0,½,½), corresponding to C_c' in *Table 3.9* of van Smaalen (2007)
[b] Values in parentheses refer to *a*, *e*, and *f* reflections respectively.

Table 3 Atomic positions and occupancies in the modulated structure. Note that all the fractional coordinates are based on ***c***=14Å unit cell, even though the number of independent atoms is the same as in albite cell (***c***=7 Å)

label	atom	Average Occ	Max Occ	Min Occ	x	y	z	Uequiv
M1	Ca	0.158(10)	0.272	0.055	0.2684(2)	-0.0116(4)	0.0793(4)	0.0302(7)
	Na	0.482(14)	0.654	0.301				
M2	Ca	0.361(10)	0.637	0.133	0.2705(2)	0.0274(2)	0.04914(16)	0.0259(6)
T1o	Si	0.4314	0.884	0.107	0.49386(3)	0.335594(18)	-0.107002(18)	0.01024(8)
	Al	0.5686	0.893	0.116				
T1m	Si	0.6888	0.954	0.250	0.50319(3)	0.317713(17)	0.116019(17)	0.00993(8)
	Al	0.3112	0.750	0.046				
T2o	Si	0.7057	0.926	0.270	0.68554(3)	0.109339(17)	0.158333(18)	0.00990(8)
	Al	0.2943	0.630	0.074				
T2m	Si	0.6585	0.921	0.203	0.18169(3)	0.379491(17)	0.178603(17)	0.00979(8)
	Al	0.3415	0.797	0.079				
Oa1	O	1			0.49795(8)	0.37147(5)	0.01117(5)	0.0183(2)
Oa2	O	1			0.58108(8)	-0.00691(4)	0.13907(5)	0.0135(2)
Obo	O	1			0.81162(8)	0.10554(5)	0.09434(5)	0.0181(2)
Obm	O	1			0.31664(8)	0.35355(5)	0.12254(6)	0.0242(3)
Oco	O	1			0.48585(8)	0.20771(5)	-0.13984(5)	0.0177(2)
Ocm	O	1			0.51473(8)	0.18895(5)	0.10770(5)	0.0179(2)
Odo	O	1			0.30164(8)	0.39259(5)	0.30849(5)	0.0173(2)
Odm	O	1			0.68998(8)	0.36705(5)	0.21565(5)	0.0211(2)

The split nature of M site is unquestionable in plagioclase, yet no conventional nomenclature of the splitting sites has been developed (Smith and Brown 1988). Most previous papers named the site with negative *y* coordinates the first site (M1, not necessarily the primary one), and the one with positive *y* coordinate the second (Fitz Gerald et al. 1986; Steurer and Jagodzinski 1988; Wenk et al. 1980; Yamamoto et al. 1984), with the exception of Boysen and Kek (2015). We follow the majority's notation in this paper and name the two M sites with negative *y* and positive *y* M1 and M2, respectively.

The importance of M site model seems to have escaped the attention of previous attempts on solving the modulated structure of intermediate plagioclase, even though detailed M sites structure has been studied extensively in the averaged structure. Yamamoto et al. (1984) refined the structure by assigning Na and Ca to both M sites, yet a few constraints were applied to force every single parameter to fall within a reasonable range. However, the refined result on M site

was not described in the paper, only the summed Ca occupational modulation wave was provided. In Boysen and Kek's (2015) paper, a model with only Na and Ca assigned to each M site respectively was used, which resulted in unrealistic occupancies (>1) and an composition obviously differ from the average structure and the real composition. The positions of atoms didn't match the electron density peaks very well either. The Na and Ca atoms were claimed to be exchangeable "without loss of fit quality", which is questionable and inconsistent with previous work (Fitz Gerald et al. 1986). This model is too simple to represent the real modulated structure despite the reported low R values.

Ordering of Ca and Na is a significant factor in the ordering-induced transformation from high intermediate plagioclase ($C\bar{1}$) to *e*-plagioclase. A model with three atoms in two M sites is used in this refinement. Only Ca was put into M2 site, but M1 contains both Ca and Na. The total occupancy of three atoms was fixed to 1. This model results in a bulk composition very close to the average structure and the analyzed result, and all occupancies modulates within the reasonable range. This model is also consistent with Fitz Gerald et al's (1986) conclusion that Ca is dominant in M2 site. The occupancy modulation of individual M site is plotted in *Fig. 3*. Although the distribution of Ca between the split sites may not be exactly accurate and probably depends on the model applied, since both positional and occupational disordering are involved, the Na occupancy which directly relates total electron density should be reliable.

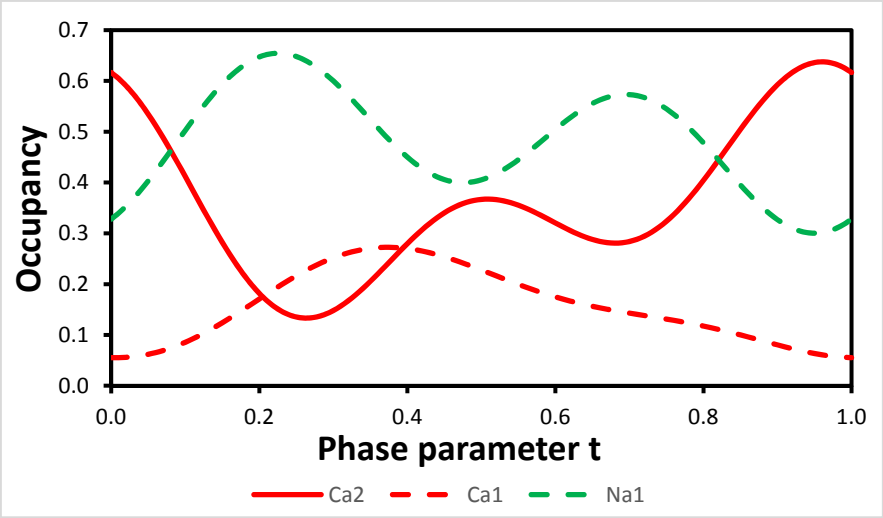

Fig. 3 Ca/Na occupancy modulation function of M site.

Since the structure factor of Al and Si are too close to be accurately refined from the data, the Al occupancy in tetrahedral sites was first fixed according to the bond distance from the average structure. Displacive modulation described by harmonic modulation functions up to second order was applied to all atoms. The M site occupancy modulation was refined to second order. All atoms were refined with harmonic ADPs with up to second order modulation. Finally, the occupancy modulation of T sites were manually entered based on the modulation of T-O bond distances (the <T-O> bond distance modulation is plotted in Fig. *4*), following the equation (Kroll and Ribbe 1983):

$$Occ(Al) = 0.25(1 + n_{An}) + (< T_i - O > - \ll T - O \gg)/k$$

The value of k is estimated to be 0.135Å from the results of Angel et al. (1990). The resulting occupancies of all sites lie in the reasonable range (between 0 and 1). The T site occupancy modulation does not affect the refinement result and is simply a direct reflection of the change in bond distance, thus freeing us from having to calculate every single T-O bond distance in the output structure. The calculated Al occupancies are considered reasonable and consistent with Ca occupancy.

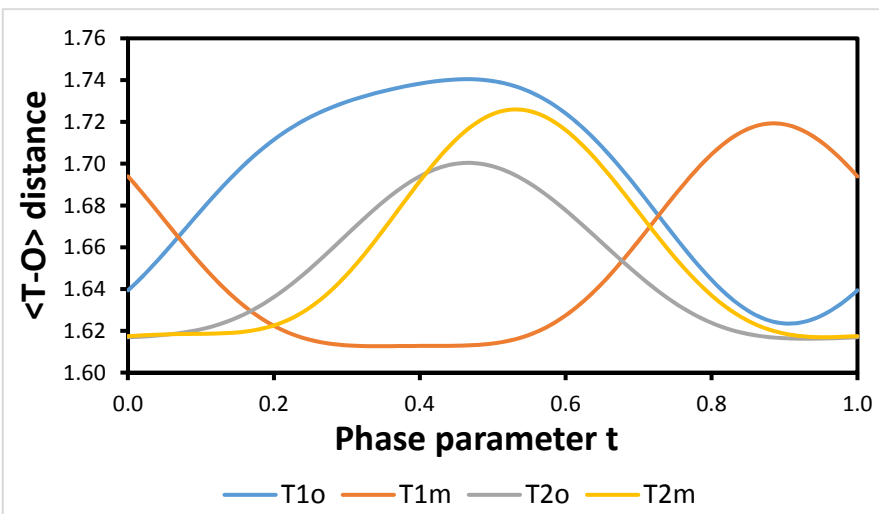

Fig. 4 T-O bond distance modulation of four T sites, the bond distance is averaged from four T-O bonds within each tetrahedron.

It's true that atomic displacement parameters (ADPs or temperature parameters) modulation increases the number of refined parameters dramatically (24 for each atom in this case), and

requires extra caution on the results of refinement as addressed by Wagner and Schoenleber (2009). However, the coordination environment for the M site is extremely complicated in plagioclase, and the temperature parameter may change a lot while the positions of atoms change. And the results were carefully checked to make sure all the atoms are vibrating within a reasonable ellipsoid. The R factor for satellite reflections dropped obviously (R value dropped from 5.04% to 2.50% for *e*-reflections, and 11.49% to 6.14% for *f*-reflections) by introducing ADP modulation. The result is consistent with the importance of applying ADP modulation addressed by Li et al (2011).

The displacement modulation of the M site happens almost entirely in the ***b-c*** plane, as the amplitude of displacement along ***a***-axis is very minor (*Fig. 5*). Therefore electron density modulation around two M sites (4 sites if we consider the splitting of each M site) is projected along ***a***-axis in *Fig. 6*. The two sites have different *x* coordinates but are put together to show the inversion relations. In the ordinary $I\bar{1}$ or $C\bar{1}$ structure for high temperature plagioclase where no modulation is involved, these two M sites are related by inversion center and should have exactly identical electron density map. However, in the modulated structure, the two M sites display polarity, as observed directly in STEM image by Xu (2015). At t=0 and t=0.5, the two M sites are related by an inversion center. If we look at the M sites on a larger scale, the two M sites together at $t=t_0$ are exactly inverted from the two M sites at $t=1-t_0$.

The displacement modulation for the splitting M site is even more interesting. The M2 site (Ca) is nearly stationary, with M1 site (Na+Ca) moving back and forth (Fig. *5*, Fig. *6*). The electron density map matches two sites model very well, showing two peaks all the time, except when the M1 site is moving too close to M2 and two peaks merge into one. Fitz Gerald et al, when solving plagioclase structures with only *a*-reflections, mentioned that a more accurate description of the M site "may require a continuum of scattering matter, or at least a series of closely spaced cation sites" (Fitz Gerald et al. 1986); Boysen and Kek (2015) also found that adding a M3 site to the average structure considerably reduced the R value. These could be result of the continuous movement of the M1 site in the modulated structure. However, the modulated structure shows no evidence of the necessity to introduce more than two splitting sites. And this behavior of M site displacement is model independent (as long as two split sites are applied). It is suggested that the occupancy of Ca in the M1 site is related to the crystal composition and structure state.

Plagioclase of the same composition with $C\bar{1}$ symmetry (like those in volcanic rocks) will have large Ca occupancy, similar to the crystal studied by Fitz Gerald et al. (1986). The transformation from $C\bar{1}$ to the modulated structure involves Ca-Na ordering besides Al-Si ordering.

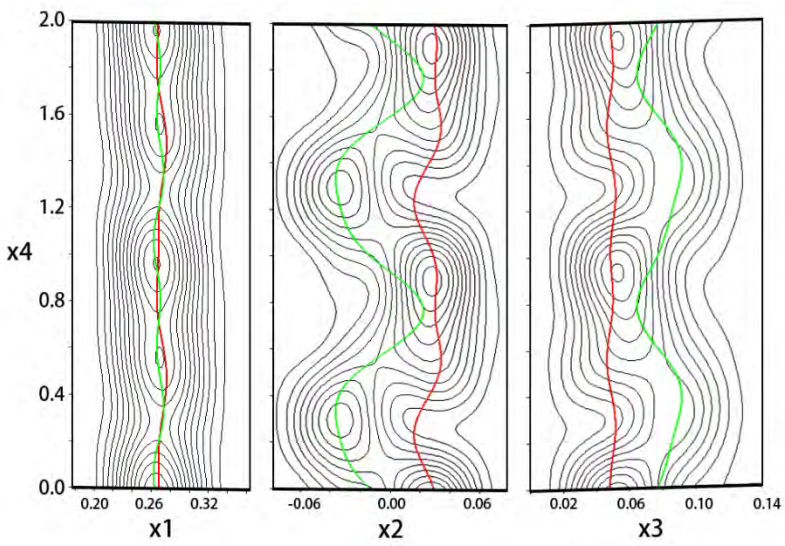

Fig. 5 The displacement modulation along ***a***, ***b***, ***c*** axis and electron density contour variation, the red line represents M2(Ca) and green line represents M1(Na+Ca), xi (i = 1, 2, 3, 4) are unit cell edge in (3+1)D space.

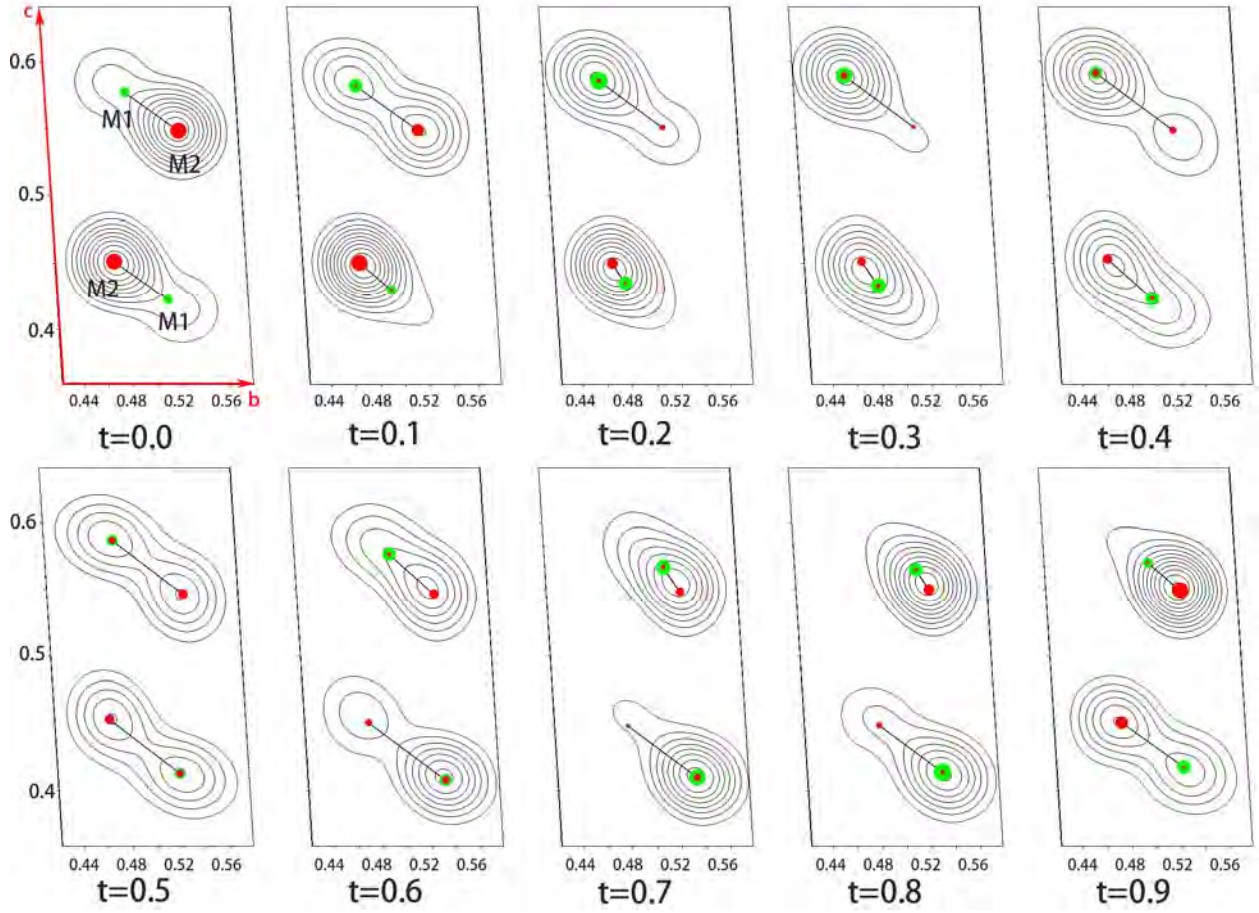

Fig. 6 Electron density map around two adjacent M site projected along ***a***-axis. The two sites have different *x* coordinates. (*Supplementary Movie 2* showing the continuous changing in electron density map is provided).

3D structure

The incommensurately modulated structure and it's (3+1)D interpretation is quite elusive to those who are not familiar with this concept. One can be easily overwhelmed by massive literature discussing the mathematical representation of the modulated structure. 775 superspace groups are found in (3+1)-dimension (Stokes et al. 2011), which is more than triple the number of the three dimensional space groups. Fortunately, plagioclase is among the structures with the lowest symmetry, therefore most of atoms are described independently. One can construct an aperiodic structure in real space given enough information without fully understanding the symmetry in (3+1)D superspace.

Just like we can't construct a 3D crystal structure given only the fractional coordinates of atoms without unit cell parameters, plotting the modulation waves on the fourth dimension won't tell what the real structure look like without combining them with a ***q***-vector. The ***q***-vector provides the information of the relation between the fourth axis and the other three. If we chose $t=t_0$ as origin, an original 3-D unit cell is constructed from all the parameters at $t=t_0$ (just take one frame at $t=t_0$ from *Supplementary Movie 1*). The next unit cell along ***a***-axis will have the structure constructed from $t=t_0+\delta h$, and the phase "jump" along ***b***- and ***c***-axis would be δk and δl respectively. The structure is aperiodic in the sense that δh, δk and δl aren't rational numbers, therefore no multiple of them is an integer.

A section of the aperiodic structure extending 3 subcells along ***b***-axis and 7 subcells along ***c***-axis is presented in *Fig. 7*. All the oxygen atoms were omitted to show the Al-Si ordering more clearly. The modulation wavefront is marked with red plane in the figure. The M sites near the red plane are approximately related by inversion symmetry. Yet clearly no part of the 3-D structure shows *I*-centering or translation along any direction.

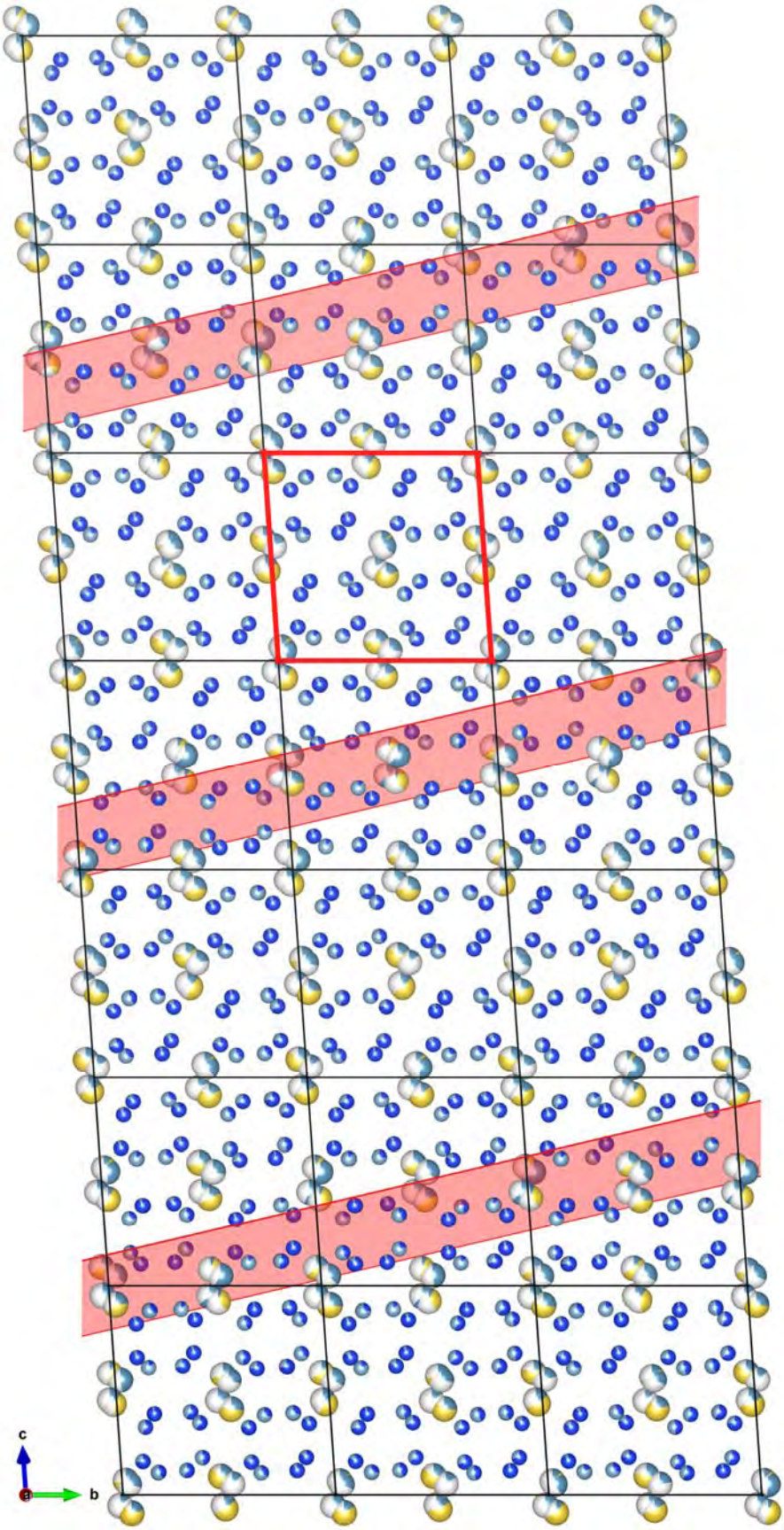

305

Fig. 7 A section of the modulated structure consists of 3x7 anorthite cells along ***b***- and ***c***-axis. The modulation wavefront is marked with red plane in the figure, which are also the section of the hyperplanes in (3+1)D structure that pass through inversion centers. Oxygen atoms are omitted. Ca/Na atoms are shown as big spheres, with blue for Ca and yellow for Na occupancies. Al/Si atoms are shown as small ones, Si occupancies are shown with dark blue color. A close-up of the red subcell is shown in *Fig. 9*.

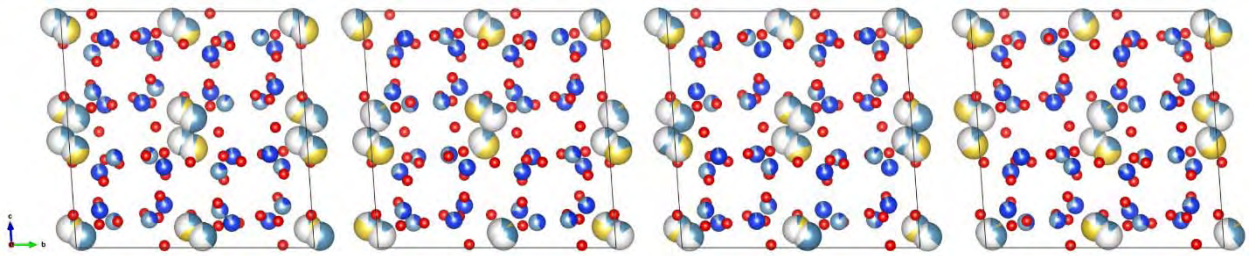

Fig. 8 Ideal anorthite cells looking down [100] at t=0, t=0.25, t=0.5 and t=0.75. These cells are produced as approximation of the subcells in real structure. The first and third model with $I\bar{1}$ symmetry represent the structure near the red planes in *Fig. 7*, while the second and fourth model with $I1$ symmetry represent the structure in the middle of two red planes. Oxygen atoms are shown as small red spheres.

If the composition of each subcell is calculated in the superstructure, a chemical variation can be observed. The subcells close to the red planes in *Fig. 7* are more Ca rich than those in the middle of two red planes. To demonstrate this trend more clearly, four anorthite cell structures corresponding to t=0, t=0.25, t=0.5 and t=0.75 are shown in *Fig. 8*. Since no three-dimensional translation symmetry is allowed in an incommensurately modulated structure, the *I*-centering unit cell is caculated from a primitive cell which represents part of the modulated structure. Therefore the unit cell shown in the *Fig. 8* is only an approximation as a whole that is convenient for comparison with a familiar anorthite cell. The chemical composition of the four cells are An59.7, An43.1, An61.5, An43.1 respectively based on Ca occupancy. The cell with inversion center is about 17 mole% higher in composition than the cells with polarity. This should indicate a density modulation with the amplitude of 17 mole% in composition. Note that the two cells of t=0.25 and t=0.75 are exactly the same structure that are related by inversion twin. (The structure

parameters of the cells in *Fig. 8* is provided in *Supplementary Data*) The two centrosymmetric cells, on the other hand, differ a little in composition, and roughly have an antiphase relation of ½***c***. This might be a reason for previously proposed "APB" models.

The Al-Si ordering shows obvious anorthite-like pattern in the Ca rich part, which is alternating Al and Si. Yet in the Na rich part of the structure, all T1o are dominated by Al, while the structure is still *I*-centered. In another word, the Na rich part shows no resemblance to an albite cell other than the fact that T1o is always rich in Al. This is consistent with NMR study of *e*-plagioclase (Kirkpatrick et al. 1987). If we take a close-up view of the fourth subcell, Most T1o sites are dominated by Al, except the lower right quarter, as a compromise for the Al avoidance rule. Interestingly, if we sum up the Al occupancy of any two adjacent T sites, none of them exceed one (the connected T1o and T1m are very close to 1 in the right half of the fourth cell), which means in the two neighboring T sites may not be occupied by Al at the same time in this structure. Average T1o occupancy is about 0.59 with average bond distance of 1.6916Å.

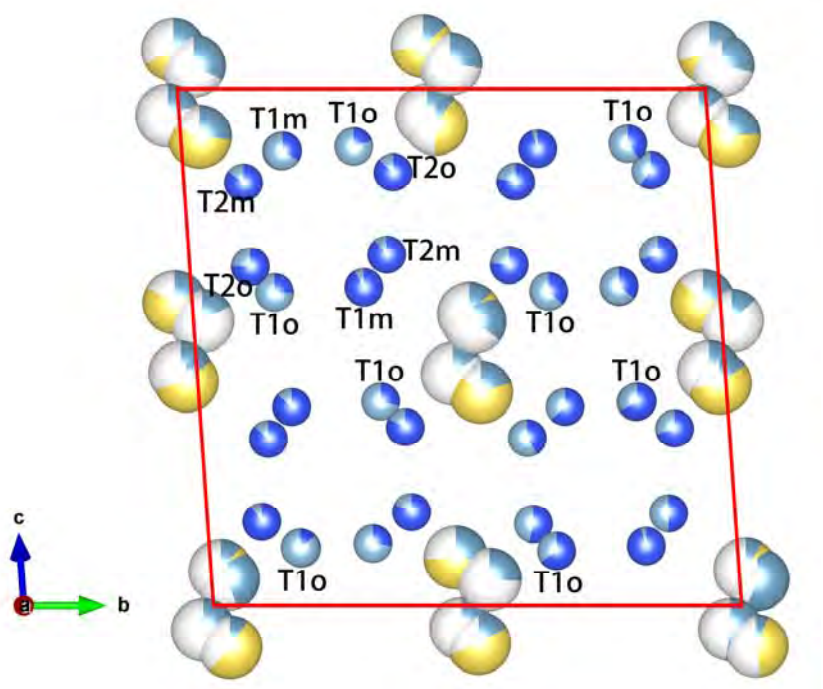

Fig. 9 A close-up view of the red subcell illustrated in *Fig. 7*.

The M site ordering is much more complicated, since two sites are involved. The distance between two splitting sites and the cation occupancy of each site both contribute to the M site

configuration, not to mention the modulated temperature parameter. There is no simplified way to describe the behavior of M site. Yet it's still reasonable to assume that the M site configuration is affected by the surrounding T site arrangement. If we look down ***b***-axis of the surrounding tetrahedra of the M site, we may find that the M site lies almost exactly on the plane defined by four surrounding T2 sites (*Fig. 10*), which is also on the (100) plane, where the major components of M site displacement modulation resides. And the splitting distance of M site obviously correlates with the shape of the quadrilateral of T2 (*Fig. 11*), as the diagonal T2 distance is shorter while two M site merge together (*Fig. 12*). The modulation of the angle T1o-Oa1-T1m is shown in *Fig. 13*, representing the distortion of the framework around M site. The two curves show maximum difference at around t=0.25 and t=0.75, and naturally, are equal at t=0 and t=0.5. Al-Si ordering results in the framework distortion and M site shifting, as well as Ca-Na ordering. Yet still there is no easy way to define any accurate formula to calculate the relationship between the two. Ca-Na ordering induced framework distortion modulation may be similar to those in incommensurately modulated nepheline (Angel et al. 2008; Friese et al. 2011), melilite (Bagautdinov et al. 2002; Bindi et al. 2001; Wei et al. 2012), and perovskite (Rusakov et al. 2011). The observed combination of tetrahedra tilts is very different from M-site induced tilts reported for monoclinic feldspars (Angel et al. 2012; Megaw 1974), because the tetrahedral tilt in the modulated structure does not change the volume of the structure. Although the angle modulation shown in *Fig. 13* is similar to type 1 tilt (Angel et al. 2012), the two angles are tilting toward opposite direction at any given point, with one inward and the other outward, introducing the polarity that cannot exist in a centrosymmetric structure.

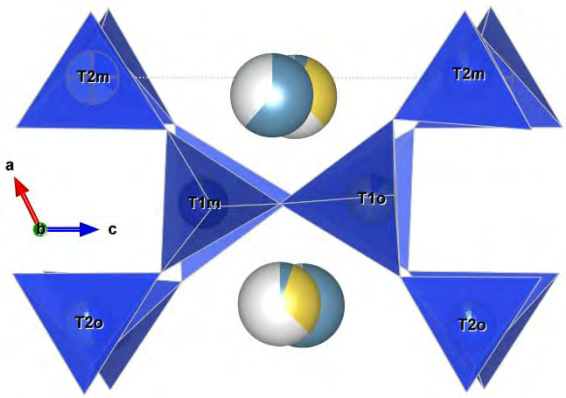

Fig. 10 Tetrahedra surrounding M sites looking down [010] (at t=0).

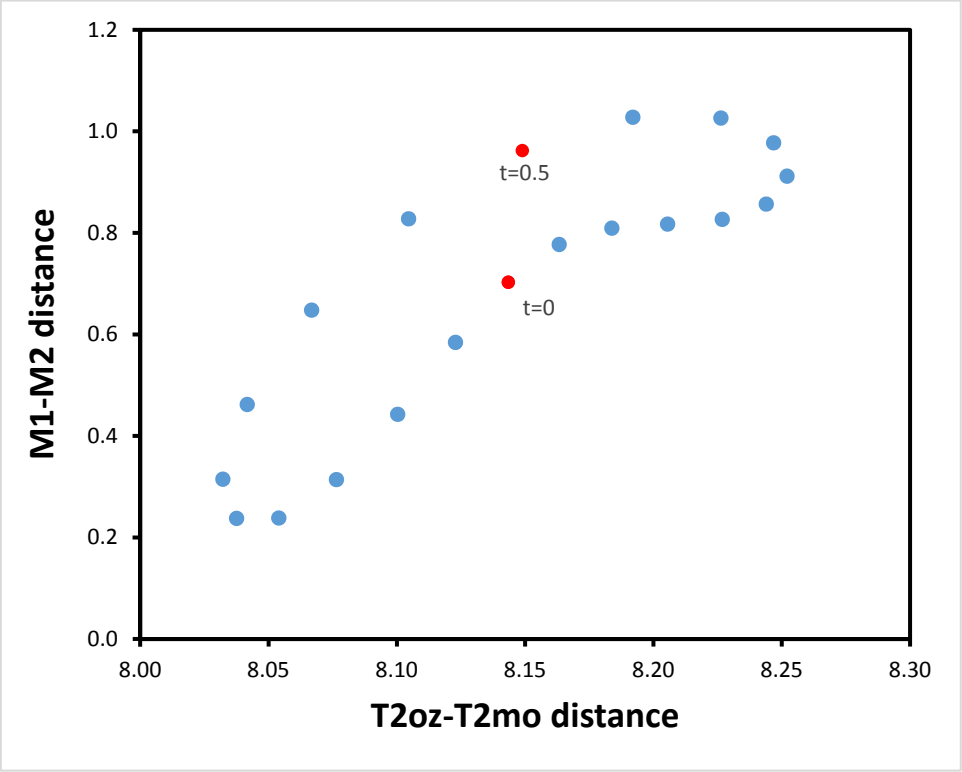

Fig. 11 Distances between M1 and M2 (splitting distance) are plotted against the corresponding T2o-T2m distances (longer diagonal of the quadrilateral). Obvious correlation between the two distance can be seen. The points labeled in red are values from the centrosymmetric cell.

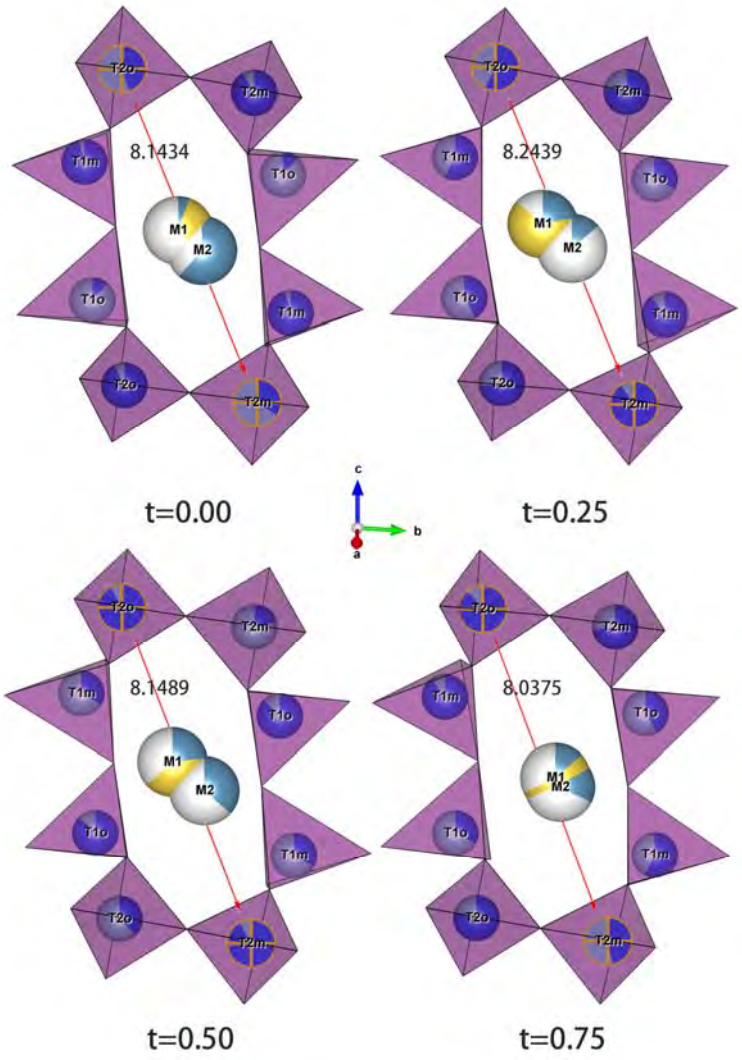

Fig. 12 M site configuration with surrounding tetrahedra at t=0, t=0.25, t=0.5 and t=0.75, looking down ***a***** perpendicular to (100) plane. Distance between diagonal T2 sites are labeled. Only the top part of *Fig. 10* is shown to avoid overlap of atoms. (*Supplementary Movie 3* showing both M sites displacement and the distortion/tilt of surrounding tetrahedra is provided.)

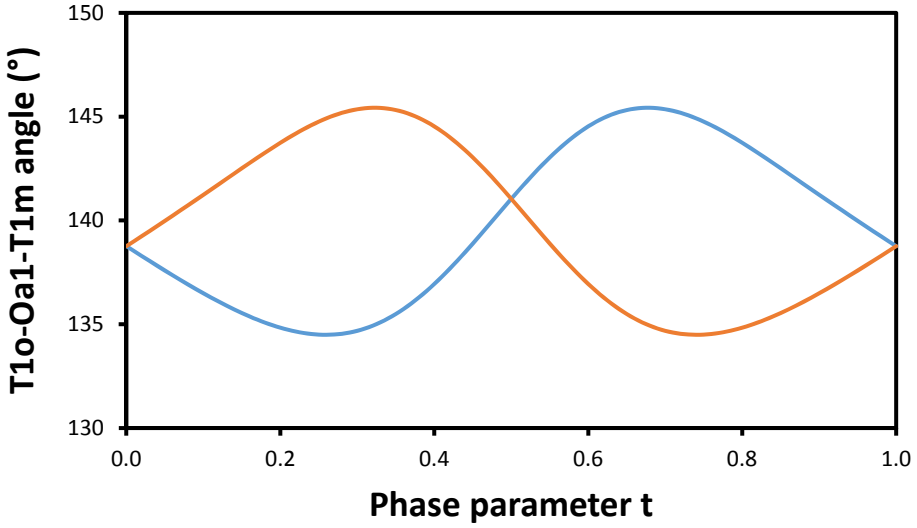

Fig. 13 The modulation of T1o-Oa1-T1m angle. There are two T1o and two T1m sites *Fig. 10* and *Fig. 12*, related by inversion center at t=0 and t=0.5, which are where two curves intersect. The unique tetrahedra tilt in *e*-plagioclase may be called *e*-tilt (the fifth type).

Discussions

Before refinement of modulated structure was possible, all *e*-plagioclase structures were refined with only *a*-reflections as an "average" structure. However, not much reliable information can be acquired from the average structure, even T-O bond distance should be treated with caution. Toman and Frueh (1973), who observed substantial improvement of agreement with a noncentrosymmetric average structure, did not even use split M site in their refinement. And with the charge flipping algorithm (Oszlanyi and Suto 2004, 2005), an approach from average structure to the modulated structure is not necessary. Since the inaccuracy of structure solved without *e*- and *f*-reflections isn't the focus of this paper, the average structure of this crystal won't be discussed in detail, because it gives partial truth with distorted picture about the intermediate plagioclase.

It seems the sample used in this study isn't the only *e*-labradorite that draws attention of mineralogists because of its homogeneity. Slimming (1976) accurately measured the position of *e*-reflections of two metamorphic *e*-labradorite from Broken Hill, Australia, with compositions of An52 and An54. Both samples lie in the composition range of Bøggild intergrowth, yet no

evidence of exsolution were mentioned. Even though TEM images weren't provided in her paper, based on the accuracy of the measurement, the samples should be homogenous with no exsolution. Carpenter (1994) addressed this phenomenon as the "perplexing" role played by potassium component in plagioclase. Nonetheless, Wenk (1979) also observed a peak around An50 in the histogram of plagioclase composition frequency, which should be zero if the solvus for Bøggild intergrowth is of normal shape. It's obvious that the labradorite studied previously is biased. Crystals with iridescent color visible to naked eye are always of igneous origin. More importantly, igneous crystals are usually large therefore much easier to handle than metamorphic ones. As labradorite that crystallized from magma has to cool down from its melting temperature and hits the solvus at Bøggild intergrowth from above, information below certain temperatures may only be revealed by metamorphic plagioclase grew directly below the solvus at low temperature. The highly ordered modulation of the sample in this study (homogeneous crystal with sharp and strong satellite reflections that fits the refinement amazingly well) should be strong evidence of the thermodynamic stability of *e*-labradorite at low temperatures. This conclusion directly leads to the loop-shaped solvus at Bøggild intergrowth, which closes at low temperatures as proposed by McConnell (2008). More samples with metamorphic origin should be studied in the future in order to reveal more details of the subsolidus phase relations around this composition.

Almost all previous models for *e*-plagioclase are based on periodic *I*-centered domains with antiphase relations to each other (Cinnamon and Bailey 1971; Grove 1977; Horst et al. 1981; Kumao et al. 1981; McConnell and Fleet 1963; Megaw 1960a, b, c; Nakajima et al. 1977; Smith and Ribbe 1969; Steurer and Jagodzinski 1988; Toman and Frueh 1976a, 1976b; Wenk and Nakajima 1980). All those models were successful in explaining the absence of *b*-reflections and the presence of *e*-reflections. However, instead of a continuous sinusoidal modulation wave, APB based model requires a crenel modulation function with rather abrupt changes between constant fragments, which requires additional theory to explain the absence of higher order satellites. The electron density map (Fig. 5) does not show any abrupt change in either positions or occupancies. The refinement was also attempted by applying crenel functions yet failed to improve the result in any criteria, which was also reported by Steurer and Jagodzinski (1988). The assumption of $I\bar{1}$ domains separated by $C\bar{1}$ boundaries is based on a skeptical foundation, since there haven't been any direct evidence of the existence of such domains in the structure.

Neither M site density maps nor T site ordering patterns can be explained by mixing $I\bar{1}$ and $C\bar{1}$ structure domains (Smith and Brown 1988).

Actually if we take a look at a 1-D modulated structure as an analog *Fig. 14*, where each unit cell consists only one atom and the modulation function has a period slightly longer than twice the subcell. The modulation function describes the occupancy variation of each atom in the structure. We can clearly see that the structure appears to be described by two identical functions with a phase difference of π. Technically, there are two modulation functions describing the structure now. If the atoms described by two functions are considered different, we get a doubled subcell with two atoms in each. Now the differences between two adjacent unit cells are very minor, therefore we can identify each individual subcell. Correspondingly, in reciprocal space, the subcell is represented by the reflection in the middle of two satellites that does not really exist. However, the case is not simpler by this change of subcell, because the two atoms in the subcell are not always ordered alternatively in the super cell. The two atoms are shifted every time two modulation functions intercept, creating a phase shift every half the period of the new modulation wave.

The case is similar in *e*-plagioclase, where the *e*-reflections are satellites of the absent *b*-reflection, so *I*-centered like subcells are identifiable in STEM image as observed by Xu (2015). However, the part where the inversion centers are observed corresponds to the intersection of two modulation waves. If we have to define a "domain" in regards to previous models, it should be the lamellae domains with polarity between two adjacent intersections. The intersection would then act as an inversion twin boundary between two *I*1 domains. This model is mentioned as a possibility by Toman and Frueh (1976a, 1976b), who explained the apparent discrepancy between centrosymmetric average structure and chiral domains, but did not treat this case with much interest as a major feature in his refinement.

It is also worth mentioning that the so called inversion twin boundary in *e*-plagioclase is artificial, in the sense that the choice of unit cell is arbitrary. Therefore the results regarding symmetry and inversion twin boundary are mathematical and independent from the choice of structure model. If we plot the M site occupancy along ***a***-axis (*Fig. 16*), a pattern similar to the 1-D analogy can be clearly observed, except the two atoms are related by inversion instead of translation.

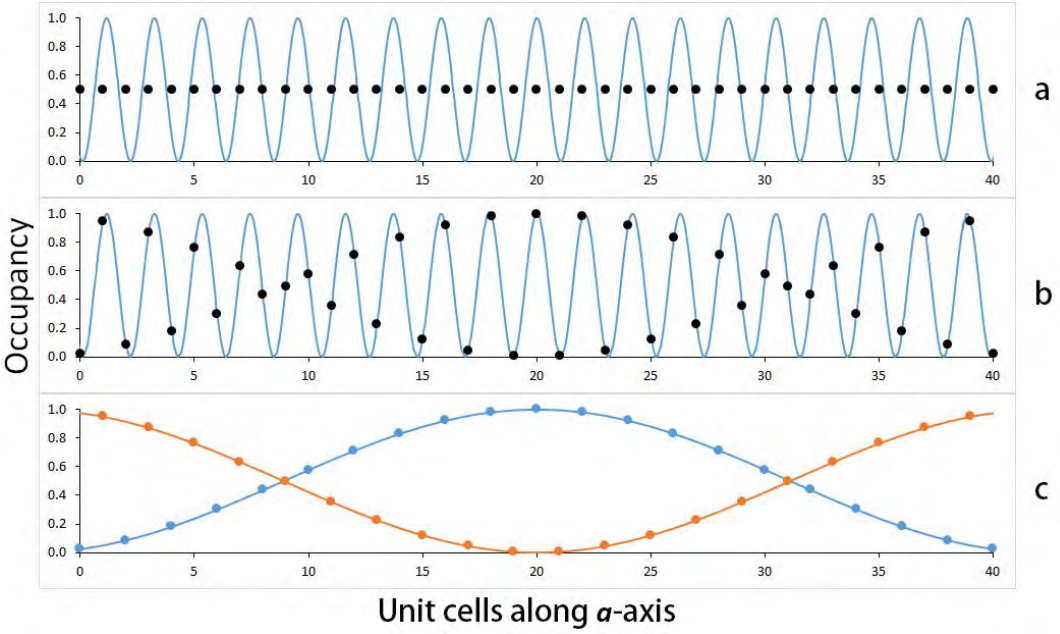

Fig. 14 1-D incommensurately modulated crystal as an analog to e-plagioclase. (**a).** normal 1-D crystal and a simple harmonic modulation wave with a period close to twice of the crystal cell. (**b).** modulated structure by superposing the crystal and the modulation wave. (**c).** same modulated structure with a different but more intuitive description, where atoms alternates between two modulation waves with longer period that are related by a phase difference of π.

Another fact we can get from 1-D analogy is that only harmonic modulation function of first order will not produce any density modulation. Since the two modulation waves are identical with phase difference of π, average of harmonic modulation function of first order would result in constant value. Only by introducing harmonic modulation function up to second, as shown in *Fig. 15*, will the structure display density modulation. This is the reason why all previous refinement without *f*-reflection did not provide any information about density modulation. Second order modulation won't cancel out because π is exactly its period. This also means it would be wrong to interpret the modulation function of any individual site as density modulation, and the first order fluctuation of occupancy in M sites represents nothing other than ordering within the unit cell.

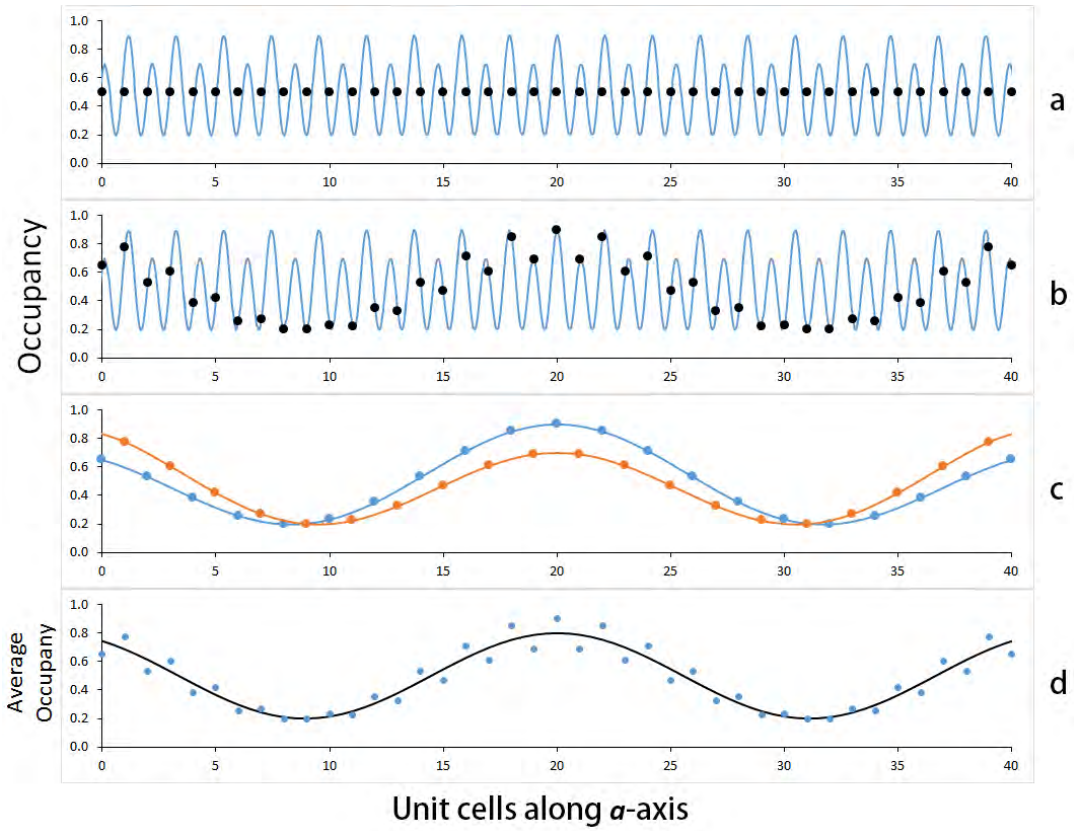

Fig. 15 By adding harmonic modulation function of second order to the 1D crystal in *Fig. 14*, the density modulation of the structure is introduced.

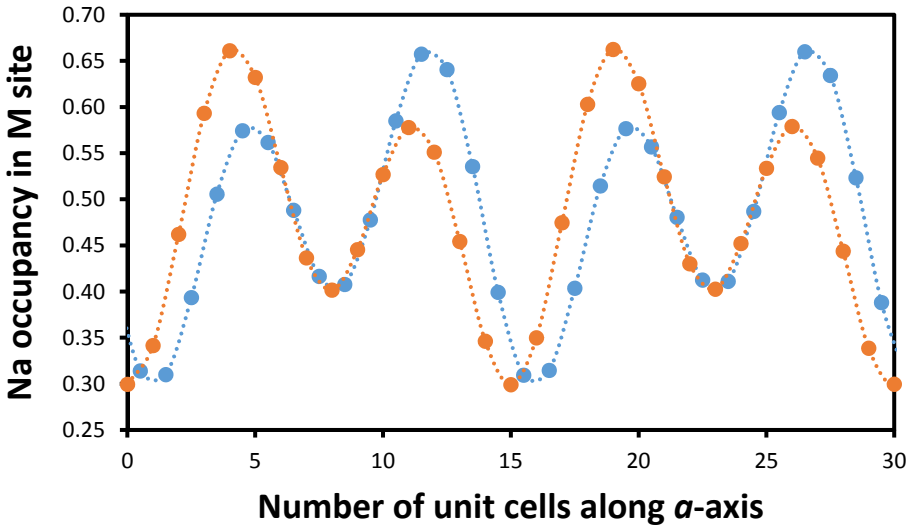

Fig. 16 Na occupancy along ***a***-axis is described by two modulation functions that are similar as in *Fig. 15*, except the alternating atoms are related by hypothetical inversion centers, instead of simple translation. Alternating atoms are marked with different color to show the trend.

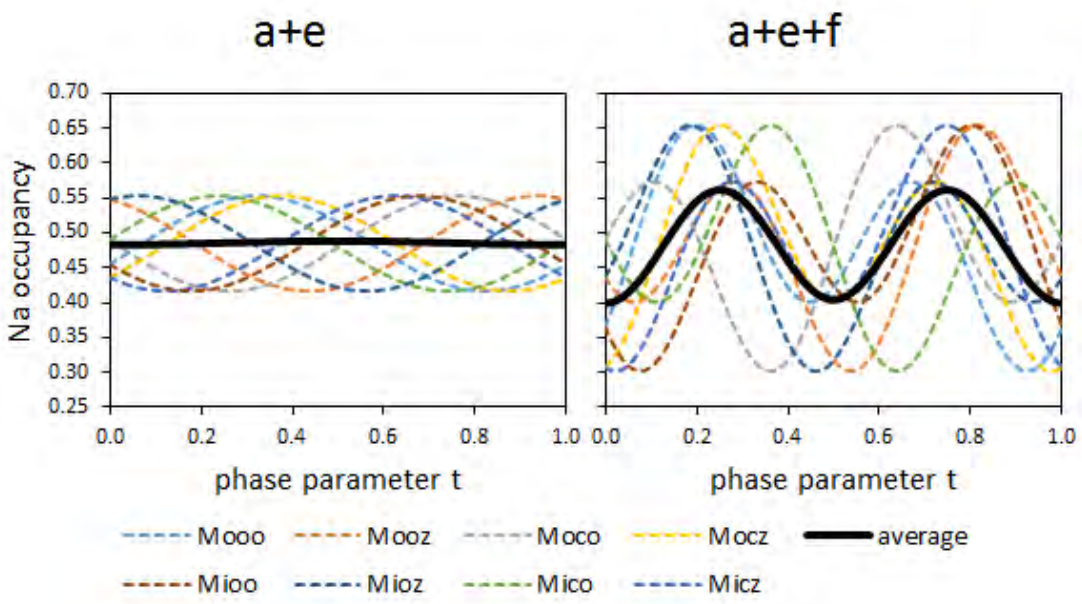

Fig. 17 Occupancy modulation of 8 symmetrically equivalent Na within one anorthite cell and there average. (**a**). only harmonic modulation function of first order refined from *a*- and *e*-reflections, the average of eight sites is constant. (**b**). up to second order modulation is refined with *a*-, *e*- and *f*-reflections, the average of eight sites shows a density modulation with an amplitude of 17 mole % of in composition change.

The 3-D structure is a little more complicated for more symmetry relations are involved. There are 8 symmetrically equivalent M sites within each anorthite cell. If the M site occupancy is refined with only harmonic modulation function of first order by neglecting *f*-reflections, the average occupancy within one subcell will be constant. But if the occupancy is refined to second order with *f*-reflections, the average occupancy will fluctuate around the averaged value (Fig. *17*). The two Na occupancy peaks have exactly the same value, since two Na rich domains are related by an inversion center. The troughs of Na occupancy modulation are slightly different since they correspond to two kinds of inversion boundaries described in the 3D structure.

This might be why two completely different models raised by Horst et al. (1981) and Yamamoto et al. (1984) could fit the exact same set of data. Critical information is lost by neglecting *f*-reflections. It is disappointing that Boysen and Kek (2015) failed to address these reflections, and kept using the modulation function of each individual atom to represent the whole structure, even though third order satellites were detected in their data.

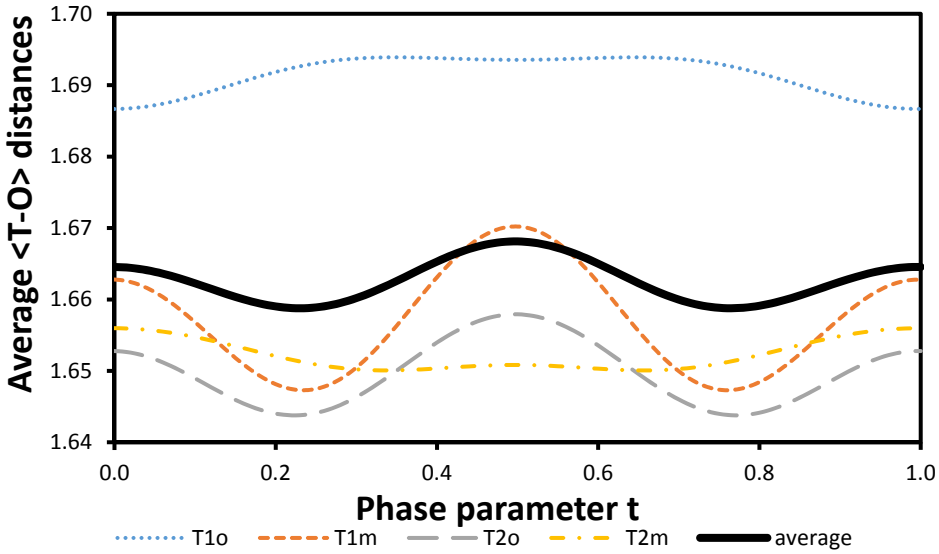

Fig. 18 Average bond distances of 8 symmetrically equivalent T sites and total average (32 sites) within one anorthite cell. Two peaks of bond distance corresponds to two Ca rich inversion boundaries.

The T-O bond distance modulation is a little different from the M site occupancy. If we average all T-O bond distances in one anorthite cell (Fig. *18*), the two peaks which correspond to two inversion boundaries respectively, shows rather obvious difference, though the two troughs of the bond distance are still the same. This might be caused by the fact that in the ideal sanidine structure, M sites are on the mirror planes and thus more symmetrical than T sites. This may also indicate the T-O bond distance is not totally reliable in predicting the Al occupancy, as local charge should be balanced in the structure with density modulation.

The average T-O bond distance for T1o, T1m, T2o and T2m are 1.6916Å, 1.6570Å, 1.6497Å and 1.6522Å respectively. The average bond distance from modulated structure is always slightly bigger than the bond distance from "average structure" refined without satellite reflections. This is because the Fourier map of *a*-reflections tends to average the modulating atom positions, and the distance of "average positions" refined without satellite reflections is always smaller than the real distances in the modulated structure. The difference may not be significant, but the plotting of T-O bond distance against An composition of plagioclase (Ribbe and Hofmeister 1983; Smith and Brown 1988) should be reexamined.

The average Al occupancy of T1o calculated from bond distance is 0.59, which is slightly larger than the occupancy of 0.5 in anorthite structure. Yet it's still dramatically smaller than the mechanical mixture of albite and anorthite structure. It is proposed that reported large enthalpy between modulated and disordered An-rich plagioclase (Carpenter et al. 1985) may be related to both Si-Al ordering, Na-Ca ordering, and density modulation. On the other hand, the observed small enthalpy between modulated and disordered Na-rich plagioclase (Carpenter et al. 1985) may be a result of Si-Al ordering without density modulation. It's still unknown how the Al/Si ordering in the *e*-plagioclase helps to lower the Gibbs free energy and make the structure more stable. Computational simulation work might be able to explain the mechanism of the T site ordering in *e*-plagioclase in the future.

Implications

The growth of the plagioclase studied in this paper occured below the temperature of phase transition between $C\bar{1}/I\bar{1}$ and *e*-plagioclase, yet the crystal is homogeneous with no exsolution

lamellae. This is an evidence of the loop shape of the solvus at Bøggild miscibility gap, as proposed by McConnell(1974; 2008). The metamorphic nature of the sample should support that *e*-plagioclase is a thermodynamically stable phase of intermediate plagioclase.

The result of the structure refinement agrees with the direct observation by Xu (2015) on an *e*-bytownite, which is $I1$ domains connected by $I\bar{1}$ inversion twin boundaries. The inversion boundary shows Al/Si ordering similar to anorthite, yet the $I1$ domains which are less in Ca display a special Al/Si ordering pattern which is not the same as albite structure. The ordering between Na and Ca is much more complicated, but seems to be coupled with the Al-Si ordering in neighboring T site. Thus the phase transition between $I\bar{1}$ and calcic *e*-plagioclase is pretty clear as addressed by Xu (2015), which is a loss of inversion center from the Al-Si ordering as well as Na-Ca ordering.

The *f*-reflections are critical in revealing the information regarding density modulation, since only satellite reflections of second order contributes to the chemical variation along the modulation. No *f*-reflections were reported for plagioclase with composition lower than ~An50, which means that density modulation may not occur in sodic plagioclase. The sample studied in this paper is close to the compositional boundary of observable *f*-reflections, however, still considerable amount of *f*-reflections are observed, and the amplitude of density modulation is rather dramatic. Unobserved *f*-reflections in Na rich plagioclase may be of very weak intensities, which could possibly be resolved by using strong X-ray beam and detector with high dynamic range. Nonetheless, this raises the question of the relation between sodic and calcic *e*-plagioclase feldspars, or so called *e*1 and *e*2 plagioclase (Carpenter 1994; McConnell 2008; Ribbe and Hofmeister 1983; Smith 1984). Careful refinement on sodic *e*-plagioclase and labradoite feldspars with different cooling histories are required to reveal the relations between $C\bar{1}$, *e*1 and *e*2 plagioclase feldspars.

Acknowledgements

This study was supported by NSF (EAR-1530614) and the NASA Astrobiology Institute (N07-5489). Authors thank Professor John Ferry for providing us the sample, and Mr. Franklin Hobbs

for reading the manuscript and providing many helpful suggestions. Authors thank Dr. Ross Angel and an anonymous reviewer for insightful discussions for helpful comments.

References

Angel, R.J., Carpenter, M.A. and Finger, L.W. (1990) Structural variation associated with compositional variation and order-disorder behavior in anorthite-rich feldspars. American Mineralogist 75(1-2), 150-162.

Angel, R.J., Gatta, G.D., Ballaran, T.B. and Carpenter, M.A. (2008) the mechanism of coupling in the modulated structure of nepheline. The Canadian Mineralogist 46, 1465-1476.

Angel, R.J., Sochalski-Kolbus, L.M. and Tribaudino, M. (2012) Tilts and tetrahedra: The origin of the anisotropy of feldspars. American Mineralogist 97(5-6), 765-778.

Bagautdinov, B., Hagiya, K., Noguchi, S., Ohmasa, M., Ikeda, N., Kusaka, K. and Iishi, K. (2002) Low-temperature studies on the two-dimensional modulations in akermanite-type crystals: $Ca_2MgSi_2O_7$ and $Ca_2ZnSi_2O_7$. Physics and Chemistry of Minerals 29(5), 346-350.

Bindi, L., Bonazzi, P., Dusek, M., Petricek, V. and Chapuis, G. (2001) Five-dimensional structure refinement of natural melilite, $(Ca_{1.89}Sr_{0.01}Na_{0.08}K_{0.02})(Mg_{0.92}Al_{0.08})(Si_{1.98}Al_{0.02})O_7$ Acta Crystallographica Section B: Structural Science 57, 739-746.

Bown, M.G. and Gay, P. (1959) The reciprocal lattice geometry of the plagioclase felspar structures. Zeitschrift für Kristallographie 111(1-6), 1-14.

Boysen, H. and Kek, S. (2015) The modulated structure of labradorite. Zeitschrift für Kristallographie 230(1), 23-36.

Carpenter, M.A. (1994) Feldspars and Their Reactions, pp. 221-269.

Carpenter, M.A., McConnell, J.D.C. and Navrotsky, A. (1985) Enthalpies of ordering in the plagioclase feldspar solid-solution. Geochimica et Cosmochimica Acta 49(4), 947-966.

Chao, S.H. and Taylor, W.H. (1940) Isomorphous Replacement and Superlattice Structures in the Plagioclase Felspars. Proceedings of the Royal Society of London A: Mathematical, Physical and Engineering Sciences 176(964), 76-87.

Cinnamon, C.G. and Bailey, S.W. (1971) Antiphase domain structure of intermediate composition plagioclase feldspars. American Mineralogist 56(7-8), 1180-1198.

Dam, B., Janner, A. and Donnay, J.D.H. (1985) Incommensurate morphology of calaverite ($AuTe_2$) crystals. Physical Review Letters 55(21), 2301-2304.

Donnay, J.D.H. (1935) Alternating axes and symmetry symbols in crystallography. Journal of the Washington Academy of Sciences 25, 476-488.

Ferry, J.M. (1980) A case study of the amount and distribution of heat and fluid during metamorphism. Contributions to Mineralogy and Petrology 71(4), 373-385.

Fitz Gerald, J.D., Parise, J.B. and Mackinnon, I.D.R. (1986) Average Structure of an An48 Plagioclase from the Hogarth Ranges. American Mineralogist 71(11-12), 1399-1408.

Friese, K., Grzechnik, A., Petricek, V., Schonleber, A., van Smaalen, S. and Morgenroth, W. (2011) Modulated structure of nepheline. Acta Crystallographica Section B: Structural Science 67, 18-29.

Grove, T.L. (1977) A periodic antiphase structure model for the intermediate plagioclases (An 33 to An 75). American Mineralogist 62(9-10), 932-941.

Grove, T.L., Ferry, J.M. and Spear, F.S. (1983) Phase-transitions and decomposition relations in calcic plagioclase. American Mineralogist 68(1-2), 41-59.

Horst, W., Tagai, T., Korekawa, M. and Jagodzinski, H. (1981) Modulated structure of a plagioclase An52: Theory and structure determination, p. 233.

Li, L., Wölfel, A., Schönleber, A., Mondal, S., Schreurs, A.M.M., Kroon-Batenburg, L.M.J. and van Smaalen, S. (2011) Modulated anharmonic ADPs are intrinsic to aperiodic crystals: a case study on incommensurate Rb(2)ZnCl(4). Acta Crystallographica Section B: Structural Science 67(Pt 3), 205-217.

Janner, A. and Janssen, T. (2015) From crystal morphology to molecular and scale crystallography. Physica Scripta 90(8), 23.

Kirkpatrick, R.J., Carpenter, M.A., Yang, W.-H. and Montez, B. (1987) ^{29}Si magic-angle NMR spectroscopy of low-temperature ordered plagioclase feldspars. Nature 325(6101), 236-238.

Kitamura, M. and Morimoto, N. (1975) The superstructure of intermediate plagioclase. Proceedings of the Japan Academy 51(6), 419-424.

Kitamura, M. and Morimoto, N. (1977) The superstructure of plagioclase feldspars. Physics and Chemistry of Minerals 1(2), 199-212.

Kroll, H. and Ribbe, P.H. (1983) Feldspar Mineralogy. Ribbe, P.H. (ed), Mineralogical Society of American.

Kumao, A., Hashimoto, H., Nissen, H.U. and Endoh, H. (1981) Ca and Na positions in labradorite feldspar as derived from high-resolution electron-microscopy and optical

diffraction. Acta Crystallographica Section A: Foundations of Crystallography 37(Mar), 229-238.

McConnell, J.D.C. (1974) The Feldspars, pp. 460-477.

McConnell, J.D.C. (2008) The origin and characteristics of the incommensurate structures in the plagioclase feldspars. The Canadian Mineralogist 46(6), 1389-1400.

McConnell, J.D.C. and Fleet, S.G. (1963) Direct electron-optical resolution of anti-phase domains in a silicate. Nature 199, 586.

Megaw, H.D. (1960a) Order and disorder. I. Theory of stacking faults and diffraction maxima, pp. 59-78, The Royal Society.

Megaw, H.D. (1960b) Order and Disorder. II. Theory of Diffraction Effects in the Intermediate Plagioclase Felspars, pp. 159-183, The Royal Society.

Megaw, H.D. (1960c) Order and disorder. III. The structure of the intermediate plagioclase felspars, pp. 184-202, The Royal Society.

Megaw, H.D. (1974) The Feldspars. MacKenzie, W.S. and Zussman, J. (eds), pp. 87-113.

Momma, K. and Izumi, F. (2011) VESTA 3 for three-dimensional visualization of crystal, volumetric and morphology data. Journal of Applied Crystallography 44(6), 1272-1276.

Nakajima, Y., Morimoto, N. and Kitamura, M. (1977) The superstructure of plagioclase feldspars. Physics and Chemistry of Minerals 225(August 1976).

Oszlanyi, G. and Suto, A. (2004) Ab initio structure solution by charge flipping. Acta Crystallographica Section A: Foundations of Crystallography 60(2), 134-141.

Oszlanyi, G. and Suto, A. (2005) Ab initio structure solution by charge flipping. II. Use of weak reflections. Acta Crystallographica Section A: Foundations of Crystallography 61(1), 147-152.

Palatinus, L. and Chapuis, G. (2007) SUPERFLIP - a computer program for the solution of crystal structures by charge flipping in arbitrary dimensions. Journal of Applied Crystallography 40(4), 786-790.

Petříček, V., Dušek, M. and Palatinus, L. (2014) Crystallographic Computing System JANA2006: General features, p. 345.

Ribbe, P.H. and Hofmeister, A.M. (1983) Feldspar Mineralogy, Mineralogical Society of American.

Rusakov, D.A., Abakumov, A.M., Yamaura, K., Belik, A.A., van Tendeloo, G. and Takayama-Muromachi, E. (2011) Structural Evolution of the $BiFeO_3$-$LaFeO_3$ System. Chemistry of Materials 23(2), 285-292.

Slimming, E.H. (1976) An electron diffraction study of some intermediate plagioclases. American Mineralogist 61(1-2), 54-59.

Smith, J.V. (1984) Feldspars and Feldspathoids, pp. 55-94, Springer.

Smith, J.V. and Brown, W.L. (1988) Feldspar Minerals, Springer-Verlag.

Smith, J.V. and Ribbe, P.H. (1969) Atomic movements in plagioclase feldspars - kinetic interpretation. Contributions to Mineralogy and Petrology 21(2), 157-&.

Smith, J.V. and Wenk, H.-R. (1983) Reinterpretation of a Verzasca plagioclase - a correction. American Mineralogist 68(7-8), 742-743.

Steurer, W. and Jagodzinski, H. (1988) The incommensurately modulated structure of an andesine (An38). Acta Crystallographica Section B: Structural Science 44(4), 344-351.

Stokes, H.T., Campbell, B.J. and van Smaalen, S. (2011) Generation of (3+ d)-dimensional superspace groups for describing the symmetry of modulated crystalline structures. Acta Crystallographica Section A: Foundations of Crystallography 67(1), 45-55.

Toman, K. and Frueh, A. (1973) on the centrosymmetry of intermediate plagioclase. Zeitschrift für Kristallographie (138), 337-342.

Toman, K. and Frueh, A.J. (1976a) Modulated structure of an intermediate plagioclase. II. Numerical results and discussion. Acta Crystallographica Section B: Structural Science 32(2), 526-538.

Toman, K. and Frueh, A.J. (1976b) Modulated structure of an intermediate plagioclase. I. Model and computation. Acta Crystallographica Section B: Structural Science 31250.

van Smaalen, S. (2007) Incommensurate crystallography, Oxford University Press, USA.

Wagner, T. and Schoenleber, A. (2009) A non-mathematical introduction to the superspace description of modulated structures. Acta Crystallographica Section B: Structural Science 65(3), 249-268.

Wei, F.X., Baikie, T., An, T., Kloc, C., Wei, J. and White, T. (2012) Crystal Chemistry of Melilite $[CaLa]_2[Ga]_2[Ga_2O_7]_2$: a Five Dimensional Solid Electrolyte. Inorganic Chemistry 51(10), 5941-5949.

Wenk, H.-R. (1979) Albite-anorthite assemblage in low-grade amphibolite facies rocks. American Mineralogist 64(11-1), 1294-1299.

Wenk, H.-R., Joswig, W., Tagai, T., Korekawa, M. and Smith, B.K. (1980) Average structure of an 62-66 labradorite. American Mineralogist 65(1-2), 81-95.

Wenk, H.-R. and Nakajima, Y. (1980) Structure, formation, and decomposition of APB's in calcic plagioclase. Physics and Chemistry of Minerals 186.

Xu, H. (2015) Direct observation of Ca-Na ordering and structure polarity in Ca-rich intermediate plagioclase feldspar with incommensurate modulated structure. American Mineralogist 100(2-3), 510-515.

Yamamoto, A., Nakazawa, H., Kitamura, M. and Morimoto, N. (1984) The Modulated Structure of Intermediate Plagioclase Feldspar Ca□Na_{1-}□Al_{1+}□Si_{3-}□O_8. Acta Crystallographica Section B: Structural Science 40(Jun), 228-237.

Fig. 1 Previously proposed models for *e*-plagioclase. ***a***. $I\bar{1}$ domains separated by antiphase boundaries; ***b***. $I\bar{1}$ domains with antiphase relation separated by albite-like $C\bar{1}$ domains, the different colors indicate compositional variation.

Fig. 2 Dark-field TEM image along ***a***-axis showing albite twin boundary (left); An selected-area electron diffraction pattern showing main *a*-reflections and satellite reflections (*e*- and *f*-reflections). No exsolution lamellae were observed in this crystal.

Fig. 3 Ca/Na occupancy modulation function of M site.

Fig. 4 T-O bond distance modulation of four T sites, the bond distance is averaged from four T-O bonds within each tetrahedron.

Fig. 5 The displacement modulation along ***a***, ***b***, ***c*** axis and electron density contour variation, the red line represents M2(Ca) and green line represents M1(Na+Ca), xi (i = 1, 2, 3, 4) are unit cell edge in (3+1)D space.

Fig. 6 Electron density map around two adjacent M site projected along ***a***-axis. The two sites have different *x* coordinates. (*Supplementary Movie 2* showing the continuous changing in electron density map is provided).

Fig. 7 A section of the modulated structure consists of 3x7 anorthite cells along ***b***- and ***c***-axis. The modulation wavefront is marked with red plane in the figure, which are also the section of the hyperplanes in (3+1)D structure that pass through inversion centers. Oxygen atoms are omitted. Ca/Na atoms are shown as big spheres, with blue for Ca and yellow for Na occupancies. Al/Si atoms are shown as small ones, Si occupancies are shown with dark blue color. A close-up of the red subcell is shown in *Fig. 9*.

Fig. 8 Ideal anorthite cells looking down [100] at t=0, t=0.25, t=0.5 and t=0.75. These cells are produced as approximation of the subcells in real structure. The first and third model with $I\bar{1}$ symmetry represent the structure near the red planes in *Fig. 7*, while the second and fourth model with $I1$ symmetry represent the structure in the middle of two red planes. Oxygen atoms are shown as small red spheres.

Fig. 9 A close-up view of the red subcell illustrated in *Fig. 7*.

Fig. 10 Tetrahedra surrounding M sites looking down [010] (at t=0).

Fig. 11 Distances between M1 and M2 (splitting distance) are plotted against the corresponding T2o-T2m distances (longer diagonal of the quadrilateral). Obvious correlation between the two distance can be seen. The points labeled in red are values from the centrosymmetric cell.

Fig. 12 M site configuration with surrounding tetrahedra at t=0, t=0.25, t=0.5 and t=0.75, looking down ***a***** perpendicular to (100) plane. Distance between diagonal T2 sites are labeled. Only the top part of *Fig. 10* is shown to avoid overlap of atoms. (*Supplementary Movie 3* showing both M sites displacement and the distortion/tilt of surrounding tetrahedra is provided.)

Fig. 13 The modulation of T1o-Oa1-T1m angle. There are two T1o and two T1m sites *Fig. 10* and *Fig. 12*, related by inversion center at t=0 and t=0.5, which are where two curves intersect. The unique tetrahedra tilt in *e*-plagioclase may be called *e*-tilt (the fifth type).

Fig. 14 1-D incommensurately modulated crystal as an analog to e-plagioclase. (**a).** normal 1-D crystal and a simple harmonic modulation wave with a period close to twice of the crystal cell. (**b).** modulated structure by superposing the crystal and the modulation wave. (**c).** same modulated structure with a different but more

intuitive description, where atoms alternates between two modulation waves with longer period that are related by a phase difference of π.

Fig. 15 By adding harmonic modulation function of second order to the 1D crystal in *Fig. 14*, the density modulation of the structure is introduced.

Fig. 16 Na occupancy along ***a***-axis is described by two modulation functions that are similar as in *Fig. 15*, except the alternating atoms are related by hypothetical inversion centers, instead of simple translation. Alternating atoms are marked with different color to show the trend.

Fig. 17 Occupancy modulation of 8 symmetrically equivalent Na within one anorthite cell and there average. (**a**). only harmonic modulation function of first order refined from *a*- and *e*- reflections, the average of eight sites is constant. (**b**). up to second order modulation is refined with *a*-, *e*- and *f*-reflections, the average of eight sites shows a density modulation with an amplitude of 17 mole % of in composition change.

Fig. 18 Average bond distances of 8 symmetrically equivalent T sites and total average (32 sites) within one anorthite cell. Two peaks of bond distance corresponds to two Ca rich inversion boundaries.